

1918

The Vanishing Shutter-Speed Limit

Ruiliang Bai¹, Charles S. Springer, Jr.², and Peter J. Basser¹

¹Section on Quantitative Imaging and Tissue Sciences, DIBGI, NICHD, National Institutes of Health, Bethesda, MD, United States, ²Advanced Imaging Research Center, Oregon Health & Science University, Portland, OR, United States

Synopsis

Dynamic-contrast-enhanced MRI (DCE-MRI) has been widely used to characterize microvasculature permeability. Recently, it was shown to reveal metabolic activity using the shutter-speed pharmacokinetic paradigm (SSP), in which steady-state intra/extracellular water exchange kinetics was incorporated into DCE-MRI data analysis. Interesting insights into DCE-MRI signals come from modeling the extravascular tissue MR signal. The questions addressed here are, "When can extravascular ¹H₂O longitudinal magnetization recovery from inversion/saturation still be described by a single-exponential process, and when can the intra/extracellular water exchange kinetics be accurately determined?"

Purpose

Dynamic-contrast-enhanced MRI (DCE-MRI) is a widely used clinical imaging tool.¹ A quantitative DCE-MRI protocol is a pharmacokinetic study. A paramagnetic contrast agent (CA) is injected intravenously and transiently extravasates only to the extracellular tissue spaces, a process described by Kety-Schmitt (KS) pharmacokinetic law (Figure 1). Interesting aspects of the analysis of DCE-MRI signals come from modeling the extravascular tissue MR signal. Typically, a tracer pharmacokinetic paradigm (TP) has been used,² where longitudinal magnetization, M , recovery from inversion/saturation is assumed to be described by an empirical single exponential process with apparent relaxation rate, R' . However, this ignores an important feature of water compartmentalization, i.e., finite steady-state exchange of intra- and extracellular water molecules.³

In 1999, two-site-exchange (2SX) expressions for steady-state intra/extracellular water exchange kinetics (Figure 1) were incorporated into DCE-MRI data analysis, via the shutter-speed pharmacokinetic paradigm (SSP).³ SSP-based analysis not only characterizes microvasculature, like TP, but also reveals cellular metabolic activity.^{4,5} In SSP models, M is described with a bi-exponential function, which could admit two MR signals with different apparent relaxation rate constants. The questions addressed here are the conditions when M relaxation can still be described as a single-exponential process and when the intra/extracellular water kinetics can still be accurately determined under SSP.

Methods

To illustrate the effects of varying $[CA_0]$ during DCE-MRI, simulations with the following 2SX parameters (Figure 1): $f_j = 0.80$, $R_{100} = 0.55 \text{ s}^{-1}$, and $r_{10} = 3.94 \text{ s}^{-1}\text{mM}^{-1}$. The values were varied from 0 to 3 s^{-1} , with 0.5 s^{-1} steps, and the $[CA_0]$ values were varied from 0 to 6 mM. The simulations were run at two different intrinsic intracellular ¹H₂O relaxation rate constants: $R_{1i} = 0.55$ and 2.00 s^{-1} . In all simulations, the small microvascular plasma (and blood) signal was ignored.

The 2SX model describes intra- and extracellular M with an empirical bi-exponential function,

$$\frac{M_0 - M(t_1)}{M_0} = (1 - \cos \alpha) \left[f'_{sm} e^{-R'_{1sm} t_1} + (1 - f'_{sm}) e^{-R'_{1lar} t_1} \right] \quad (1)$$

where $M(t_1)$ is the magnetization at recovery time t_1 , M_0 , at equilibrium, α the effective flip angle of the inversion/saturation pulse, and R'_{1sm} and R'_{1lar} are the small and large apparent relaxation rate constants, respectively, and f'_{sm} is the apparent fractional intensity of the signal with R'_{1sm} . The analytical expressions for Eq. (1) quantities given in terms of physical quantities are described in Figure 2.⁶

Results

Figures

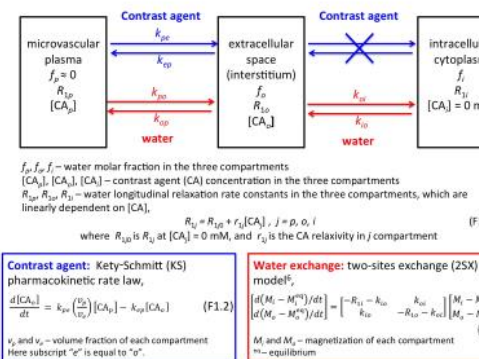


Figure 1. Shutter-Speed Pharmacokinetic Paradigm for DCE-MRI

$$R'_{1sm} = \frac{R_{1i} + R_{10} + k_{i0} + k_{0i} - \sqrt{(R_{1i} - R_{10} + k_{i0} - k_{0i})^2 + 4k_{i0}k_{0i}}}{2} \quad (F3)$$

$$R'_{1lar} = \frac{R_{1i} + R_{10} + k_{i0} + k_{0i} + \sqrt{(R_{1i} - R_{10} + k_{i0} - k_{0i})^2 + 4k_{i0}k_{0i}}}{2} \quad (F4)$$

$$f'_{sm} = \frac{(R_{10} + k_{i0} + k_{0i} - R'_{1sm})f_i - (-R'_{1lar} + R_{10})(1 - f_i)}{R'_{1lar} - R'_{1sm}} \quad (F5)$$

Figure 2. Analytical solution for the 2SX model.

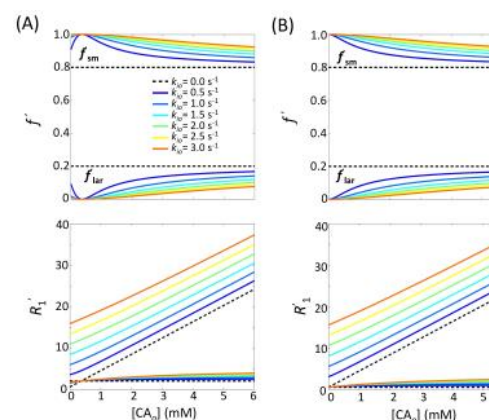


Figure 3. Analytical 2SX solutions of the empirical f'_{sm} and f'_{lar} , the relative apparent fractions of the R'_{1sm} and R'_{1lar} (up), and the apparent relaxation rate constants R'_{1sm} and R'_{1lar} themselves (down) at various $[CA_0]$ and k_{i0} values, for $\kappa_1 \equiv |R_{1i} - R_{100}| = 1.45 \text{ s}^{-1}$ (A) and 0 s^{-1} (B).

The analytical 2SX solutions for f'_{sm} , R'_{1sm} , and R'_{1lar} as functions of $[CA_o]$ and k_{io} are illustrated in **Figure 3**. Without any exchange, both f'_{sm} and R'_{1sm} are $[CA]$ -independent (horizontal dashed lines). With exchange, both parameters are strongly dependent on $[CA_o]$ and k_{io} values. For $R_{1i} - R_{1o0} = 0 \text{ s}^{-1}$, f'_{sm} is equal to 1.0 at $[CA_o] = 0 \text{ mM}$ for any finite k_{io} value. For $R_{1i} - R_{1o0} = 1.45 \text{ s}^{-1}$, f'_{sm} approaches 1.0 at $[CA_o] = 0.37 \text{ mM}$ ($R_{1i} - R_{1o0} = 0 \text{ s}^{-1}$) for any finite k_{io} value. In both cases, the recovery time-course could be well approximated with the single-exponential expression Eq. (1) with R'_1 .

Discussions

Figure 3 illustrates important theoretical features of the 2SX model. The abscissa is a measure of the longitudinal shutter-speed ($\kappa_1 \equiv R_{1i} - R_{1o0}$) for this system.⁷ For simulations at $R_{1i} - R_{1o0} = 0$ and 1.45 s^{-1} , f'_{lar} approaches 0 as κ_1 approaches zero. This has been traditionally called the fast-exchange-limit [FXL]. However, the FXL term comes from NMR in chemistry, where reactions can be accelerated or slowed, *i.e.*, k_{io} can be increased or decreased, respectively. **Figure 3** makes clear the f'_{lar} vanishing is independent of the k_{io} value at finite k_{io} . Thus, the FXL label is misleading. It is more descriptive to refer to the left ordinate as the vanishing-shutter-speed-limit [VSSL]. This is important because the TP represents a special case of the SSP – in the limit of a short SS. It has been shown algebraically that as κ_1 vanishes, R'_{1sm} approaches the f -weighted R_{1i} , R_{1o} average [$\equiv R'_1$].⁸ Any DCE-MRI model within the TP is the special VSSL case of the analogous shutter-speed model.^{7,9}

In most practical situations, $(R_{1i} - R_{1o0})$ is small in tissue but > 0 and $[CA_o]_{\max}$ rarely exceeds 2 mM.^{8,10} In these cases, f'_{lar} is very small, and its signal also likely suffers disproportionate transverse relaxation quenching ($R_{2lar}^* > R_{2sm}^*$).⁷ Thus, the component can reasonably be neglected. In this very common regime, the recovery is mono-exponential, but the relaxation rate constant is R'_{1sm} (**Figure 2**), not R'_1 defined in TP model

$$R'_1 = r_{1o}[CA_o] + R'_{1o} \quad (2)$$

This can be called the vanishing shutter-speed regime [VSSR]. Measurements in blood suggests the VSSR extends to $[CA_o]$ past 20 mM; most likely due to transverse quenching.⁸ This is important because k_{io} is only accessible in the VSSR but not the VSSL.

Acknowledgements

This work was supported by the Intramural Research Program (IRP) of the *Eunice Kennedy Shriver* National Institute of Child Health and Human Development, National Institutes of Health. Charles S. Springer, Jr. is supported by the National Institutes of Health under Awards No. UO1-CA154602 and R44-CA180425

References

1. Padhani AR. Dynamic contrast-enhanced MRI in clinical oncology: Current status and future directions. *J Magn Reson Imaging*. 2002;16(4):407-422.
2. Sourbron SP, Buckley DL. Classic models for dynamic contrast-enhanced MRI. *NMR Biomed*. 2013;26(8):1004-1027.
3. Landis CS, Li X, Telang FW, et al. Equilibrium transcytolemmal water-exchange kinetics in skeletal muscle in vivo. *Magn Reson Med*. 1999;42(3):467-478.
4. Zhang Y, Poirier-Quinot M, Springer CS, Balschi J a. Active trans-plasma membrane water cycling in yeast is revealed by NMR. *Biophys J*. 2011;101(11):2833-2842.
5. Springer CS, Li X, Tudorica LA, et al. Intratumor mapping of intracellular water lifetime: metabolic images of breast cancer? *NMR Biomed*. 2014;27:760-773
6. Bai R, Benjamini D, Cheng J, Basser PJ. Fast, accurate 2D-MR relaxation exchange spectroscopy (REXS): Beyond compressed sensing. *J Chem Phys*. 2016;145(15):154202.
7. Li X, Cai Y, Moloney B, et al. Relative sensitivities of DCE-MRI pharmacokinetic parameters to arterial input function (AIF) scaling. *J Magn Reson*. 2016;269:104-112.

8. Wilson GJ, Woods M, Springer CS, Bastawrous S, Bhargava P, Maki JH. Human whole-blood (1)H₂O longitudinal relaxation with normal and high-relaxivity contrast reagents: influence of trans-cell-membrane water exchange. *Magn Reson Med.* 2014;72(6):1746-1754.
9. Ackerman JJH. The shutter-speed paradigm: not your father's DCE-MRI. *NMR Biomed.* 2016;29(1):4-5.
10. Landis CS, Li X, Telang FW, et al. Determination of the MRI contrast agent concentration time course in vivo following bolus injection: effect of equilibrium transcytolemmal water exchange. *Magn Reson Med.* 2000;44(4):563-574.